Mineralogical Magazine, December 1998, Vol. 62(6), pp. 783–792

Correction of geometric errors associated with the 3-D reconstruction of geological materials by precision serial lapping

R. MARSCHALLINGER

Inst. für Geologie und Paläontologie, Universität Salzburg, Hellbrunnerstr. 34/III A-5020 Salzburg, Austria

ABSTRACT

Precision serial lapping in combination with raster image acquisition is an efficient and versatile approach to 3-D microstructure reconstruction of geological materials. However, during associated sample preparation and data acquisition, geometric inaccuracies are introduced, which, if neglected, severely distort the desired 3-D models of minerals and rock fabrics. A novel method is presented to assess and correct the relative shifts and rotations between the images acquired at the individual erosion levels. The method relies on optical reflection prisms which provide a precise internal reference system that allows all images making up an erosion series to be registered on a common system of coordinates. Tested on a microanalyser with digital sample stage control, the method yielded position errors between successive images of approximately 1 μm. A thorough description of the mechanical design of the reference system and the coordinate transformation formulae are given.

KEYWORDS: geological materials, 3-D microstructure, precision serial lapping, raster image acquisition.

Introduction

THE power of computer-aided 3-D reconstruction of geological materials is being increasingly recognized in the scientific as well as in the economic realm (e.g. Grunsky *et al.*, 1980; Ohashi, 1992; Marschallinger *et al.*, 1992; Johnson, 1993; Cooper and Hunter, 1995; Denison and Carlson, 1997). For microstructure reconstruction, precision serial lapping in conjunction with data acquisition by a scanning electron microscope (SEM) or an electron probe microanalyser (EPMA) is a highly versatile approach. The rock sample is eroded in constant, plan-parallel increments with a precision lapping device. Depending on the size and morphological complexity of the minerals to be reconstructed, erosion increments may range from a few microns to some hundred microns. After each erosion step, the newly created surface is scanned and the resulting image stored. Usually this is a low magnification backscattered electron image (BSI) conveying mineral phase distributions (Fig. 1); if EPMA is available, cathodoluminescence images or X-ray maps depicting quantitative chemical variations can also be acquired. By stacking the individual images and applying 3-D reconstruction algorithms, 3-D morphology and chemical variation of minerals or fabric features of interest can be modelled and submitted to analysis and viewing.

3-D reconstruction by precision serial lapping is straightforward and universal in principle, but its practical implementation requires consideration of the need to minimize geometric inaccuracies introduced during the sample preparation and data acquisition cycle. The following example illustrates the need for geometrical precision. The BSI in Fig. 1 comprises 1024 × 1024 pixels and covers a sample area of 1.575 mm side length (EPMA magnification setting ×55); the associated geometrical resolution is 1.54 μm per pixel. For distortion-free 3-D reconstruction from a series of stacked images like Fig. 1, precision of $x-y$ alignment of successive image centres must be better than 1.54 μm.

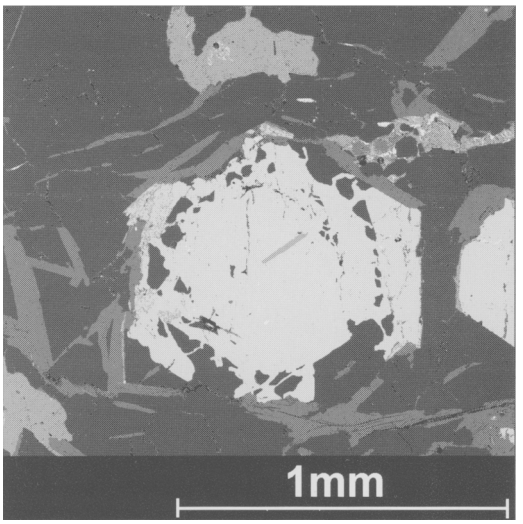

FIG. 1. Backscattered electron image (BSI) of garnet mica schist fabric; the hypidiomorphic garnet at the centre is the subject of 3-D reconstruction. Mineral phases present: small white specks are ilmenite, bright colours indicate garnet, light grey is chlorite, dark grey clots are muscovite, dark grains are quartz. Concentric, quartz inclusion-rich zones in garnet indicate discontinuous growth history. ×55 SEM magnification, 512 × 512 pixels, spectral resolution 8 bit.

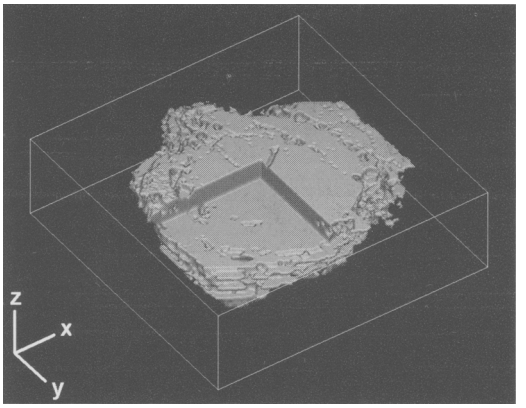

FIG. 2. 3-D visualization of garnet phase boundary (top slice as depicted in Fig. 1) in which the underlying 3-D model was reconstructed from non-rectified precision serial lapping data in which BSIs from 23 erosion levels were stacked without coordinate registration. Stair-shaped offsets of 3-D model indicate strong geometrical distortion parallel to x–y plane of the model. A rectangular portion has been removed from the garnet model for inspection of its interior; since x–y shifts between adjacent erosion levels are larger than most inclusions, related holes in garnet cannot be consistently traced in z-direction and finish abruptly at neighbouring erosion levels. Model dimensions (surrounding box, $x \times y \times z$) : 1.11 × 1.02 × 0.32 mm.

The overall geometric distortion encountered during 3-D reconstruction by precision serial lapping stems mainly from three sources: (i) lapping shift acting in the z-direction, (ii) image shift, and (iii) sample shift both acting in the x and y directions, i.e. in the erosion plane (coordinate system directions, see Fig. 2). Lapping shift, caused by unequal and nonparallel erosion intervals, is related to the mechanical design and the calibration of the lapping device and is not considered in detail here (see relevant precision parameters below). Image shift is introduced because rock-forming minerals and fabric features in geological materials generally possess a highly irregular, unpredictable morphology: even after eroding a minute interval of a few μm, the image centre of the previous erosion level cannot be precisely relocated on a newly acquired sample surface by either visual comparison or image processing techniques. Fortunately, modern SEMs and EPMAs are equipped with a digitally controlled sample stage with $x,y,(z)$ coordinate readout precision of 0.1 μm and position errors <1 μm. Since image centres can be calibrated to the stage coordinate system, successive images can be registered initially by means of stage coordinates. However, the alignment of stage coordinates will be distorted by sample shifts which arise during 3-D reconstruction by destructive lapping, because the rock sample has to be cycled between the lapping device and the image acquisition device. Since it is practically impossible to remount the sample after each erosion step at exactly the same location on the SEM's or the EPMA's sample stage, the stage x–y coordinate readouts are inconsistent between different erosion levels. Neglect of these shifts introduces severe geometrical distortions into the derived 3-D reconstructions as seen in Fig. 2.

The only practicable way to assess and correct such geometrical distortions is by means of a sample-internal reference system which remains in focus during all the erosion/acquisition cycles;

by means of this reference system, the stage coordinates of all erosion levels can be related to a common coordinate system which is bound to an arbitrarily choosen 'reference' erosion level.

Some designs for coordinate registering during destructive 3-D reconstruction have been published; one way (Marschallinger *et al.*, 1993) is to mount the sample chip on a glass specimen holder. Two reference marks are cut into the glass, the *x,y* coordinates of which are recorded at each acquisition step in order to relate all images to one reference system. Though straightforward, this method precludes an initial sample thickness larger than the acquisition device's focus range (for EPMA ~2 mm) since the sample surface as well as the specimen glass surface have to be within this range. Bryon *et al.* (1995) used a different approach, eliminating the sample thickness restriction by cutting surfaces in the sample itself at mutually perpendicular angles to create edges which are perpendicular to the erosion planes. The *x,y* locations of these edges remain constant with respect to the sample surface during the whole erosion series. They can be recorded on each erosion level and thus serve as control points for image registration. However, the disadvantage of this approach is the necessity for a specialized device to cut rock samples at perpendicular angles with sufficient precision.

A novel, conceptually simple and easy-to-implement though highly precise referencing method for serial lapping has been developed during the course of a project dealing with the 3-D microstructure reconstruction of geological materials. Based on using two optical prisms as the reference system, it enables a stage-coordinate related image registration with $x-y$ errors of approximately one micron. For each erosion level, the centre of the image to be acquired needs only to be coarsely located by eye. Corrections for image and sample shifts are performed after acquisition by means of the correction parameters yielded by the optical prism reference system. The underlying mechanical design, the derivation of suitable correction procedures and the practical application of this method are considered in detail below.

Equipment used

Precision serial lapping was performed with a Logitech CL30 compact lapping system and a Logitech PP5 GT precision lapping head. For lapping, a cast iron plate calibrated to ± 1 µm plate flatness was used; lapping agent was 3 µm calcined aluminium oxide powder. A polyurethane plate with polishing fluid SF1 was used for polishing. The reference system was assembled from Spindler & Hoyer optical reflection prisms. Images were acquired on a JEOL 8600/LINK EXL computer-controlled electron probe microanalyser. Image processing, coordinate registration, 3-D modelling and visualization were implemented in the IDL rel. 4 (Research Systems, 1995) image and data analysis and visualization package operating on a SUN/SPARC5 with 128 MB memory.

Design and application of the proposed reference system

Optical reflection prisms as reference objects

Triangular optical reflection prisms are ideal objects from which a sample-internal reference system can be assembled. They are available with a 90° angle between the base and the prismoidal faces; they are manufactured in different sizes and with different levels of angular tolerances and thus can be selected to fit sample dimensions and desired 3-D reconstruction precision. The grinding hardness of glass is within the range of most rock-forming minerals. Last but not least, since they are manufactured in large numbers, reflection prisms are comparatively inexpensive.

To set up a sample-internal reference system, two reflection prisms and the rock sample(s) are mounted on a glass plate as indicated in Fig. 3 (see also for nomenclature). Before 3-D reconstruction starts, the sample and the prisms have to be lapped until a common, plan-parallel upper surface ('s3' in Fig. 3) is achieved. Then, during 3-D reconstruction, on each serial erosion level the prism's triangular profile traces $t1-t3$, $t4-t6$ can be recorded since they lie in exactly the same focus level as the sample surface (compare also with Fig. 4). From the intersection of traces $t1-t3$ and $t4-t6$ the triangle corner points ($p1-p3$, $p4-p6$) are calculated. Since these corner points lie on the prism's edges ($e1-e3$, $e4-e6$) which are perpendicular to the glass specimen holder surfaces, this procedure yields three control points per prism (i.e. six control points per erosion level). These control points are used for coordinate registration of all erosion levels by polynomial transformation. The centres of gravity of the triangles ($g1$,$g2$) are used to assess sample rotation in any erosion level for later image-internal correction of rotation.

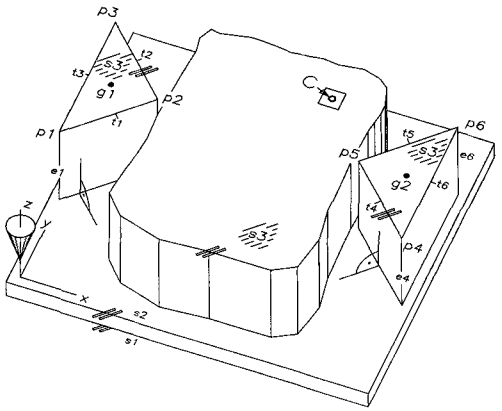

FIG. 3. Mechanical assembly of proposed reference system. Reflection prisms and rock sample are mounted on a glass specimen holder. C is the centre point of the image to be acquired. The surface subject to precision serial erosion and imaging is 's3'. During lapping, the lower surface of the glass holder ($s1$) is attached to the vacuum chuck of the precision lapping head. Notice plan-parallel surfaces $s1$, $s2$ and $s3$ as well as rectangular configuration of these surfaces and the vertical prism faces. Lapping direction is $-z$, as indicated by the cone on the z-axis. Dimensions of the assembly are approximately 5 × 5 × 2 cm. See text for details.

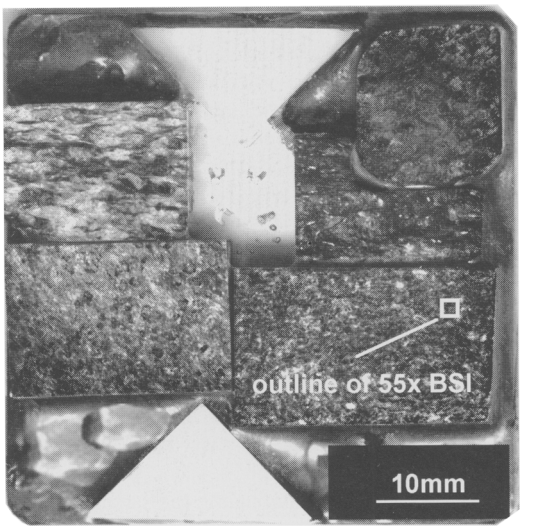

FIG. 4. Photograph of rock samples and reflection prisms mounted on a 5 × 5 cm large glass holder, plan view (compare to Fig. 3). The square, white outline depicts the area covered by a BSI acquired at 55-times magnification. To make the sample preparation and data acquisition cycle as efficient as possible, five rock samples and four micropalaeonological samples were mounted on one glass holder; in this arrangement, 37 BSIs were acquired per erosion level.

Deducing control points

On the reflection prisms, edges $e1-e6$ are chamfered at the factory to avoid injury or splintering (see insert to Fig. 5); thus, 'virtual' corner points $p1-p3$, $p4-p6$ have to be calculated by intersecting the lines deduced from the visible triangle edges, $t1-t3$ and $t4-t6$. Though more complicated than simply extracting coordinates of physically existing corner points, this indirect approach enhances the overall precision of the reference system. Picking the stage coordinates of more than 2 points per edge enables the use of linear regression to calculate $t1-t6$ as best fit lines (Fig. 5). Regression lines can be straightforwardly calculated from stage coordinate readouts (eq. 1, regression after Rock, 1988):

$$k = \frac{\sum_{n=1}^{n}\left(x_n - \bar{x}\right)\left(y_n - \bar{y}\right)}{\sum_{n=1}^{n}\left(x - \bar{x}\right)^2}; d = \bar{y} - k\bar{x}; y = kx + d \qquad (1)$$

where n is the number of points picked per edge $t1-t6$, x_n, y_n are the stage coordinate x, y readouts of point n and $\bar{x}$ and $\bar{y}$ are the means. Setting up linear equations (eq. 1c) for each edge ($t1$, $t2$, $t3$) and solving the simultaneous equations $t1-t3$, $t1-t2$ and $t2-t3$ yields x,y coordinates respectively for $p1$, $p2$, $p3$ (similarly for $p4-p6$).

Correction for sample shift

Polynomial transformation is a universal method to register coordinate systems. Depending on the order of the polynomial, translation, rotation, scaling, shearing and rubber sheet warping are possible (Mather, 1989). For geological materials their rigidity precludes deformation by the preparation process. Therefore, all geometrical inaccuracies introduced during the preparation/acquisition cycle are amenable to correction by translation and rotation. In this context, a first-order polynomial accomplishes both translation and rotation of image centre points.

Practically, polynomial transformation relies on a set of control points which can be identified in the coordinate systems to be registered. Figure 6

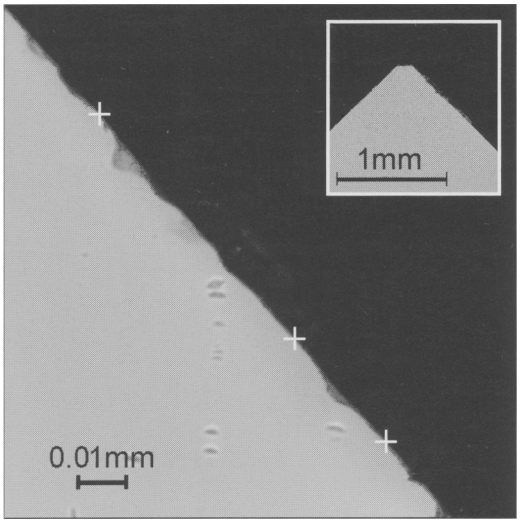

FIG. 5. Details of reflection prism edges ($t1-t6$) as viewed in backscattered electron mode (BSI magnification 450 x). During lapping, at the erosion interface ($s3$), prism edges $t1-t6$ are subject to splintering at the microscopic scale. However, sufficient prism edges remain undamaged to allow exact stage coordinate picking (white crosshairs) for recalculation of prism edges as best fit lines (eq. 1). The BSI inserted at the upper right corner shows a chamfered prism edge; therefore, prism edges $e1-e6$ have to be calculated (magnification of insert 55 ×).

depicts the application of polynomial transformation to the current problem. Consider, constructed from stage coordinate readouts on the reference erosion level, the two triangles made up of control points $p1-p3$ and $p4-p6$ (compare Fig. 3) as well as the reference image centre point, labelled C. Removing the sample from the acquisition device's sample stage, and then lapping and remounting it on the sample stage will introduce a position shift with respect to the absolute stage coordinate system. This shift will be expressed by a different location of the triangles ($p1'-p3'$, $p4'-p6'$) as well as the centre of the newly acquired image (c', the location of which is additionally biased by image shift, see below). The polynomial coefficients are derived from the coordinate differences of control point pairs $p1-p1'$, ... , $p6-p6'$. By solving the polynomial equations, the centre point c' of an image acquired at an arbitrary erosion level can be transformed to the coordinate system of the reference erosion level (c''). To solve a first-order polynomial (eq. 2):

$$\begin{aligned} x_1 &= a_{00} + a_{10}x_2 + a_{01}y_2 \\ y_1 &= b_{00} + b_{10}x_2 + b_{01}y_2 \end{aligned} \qquad (2)$$

at least three pairs of control points are necessary, where $x1,y1$ and $x2,y2$ are the coordinates of a control point in the reference and in the distorted coordinate systems, and a_{00}, a_{10}, a_{01}, b_{00}, b_{10}, b_{01} are the polynomial coefficients. Since the triangular sections of the two prisms contribute 6 control points per erosion level, the system of equations (2) is overdetermined, and, by least-squares technique (Göpfert, 1987), the polynomial coefficients can be evaluated on a statistical basis (summarized as eq. 3):

$$\begin{aligned} \sum &= \sum_{n=1}^{n} \\ x_{is} &= \sum x_i/n; \qquad y_{is} = \sum y_i/n \\ & \qquad\qquad\qquad\qquad \}i = 1,2 \\ X_i &= x_i - x_{is}; \qquad Y_i = y_i - y_{is} \\ D &= \sum X_2^2 \sum Y_2^2 - \left(\sum X_2 Y_2\right)^2 \\ a_{10} &= \left(\sum Y_2^2 \sum X_2 X_1 - \sum X_2 Y_2 \sum Y_2 X_1\right)/D \\ a_{01} &= \left(\sum X_2^2 \sum Y_2 X_1 - \sum X_2 Y_2 \sum X_2 X_1\right)/D \\ a_{00} &= x_{1s} - a_{10}x_{2s} - a_{01}y_{2s} \\ b_{10} &= \left(\sum Y_2^2 \sum X_2 X_1 - \sum X_2 Y_2 \sum Y_2 Y_1\right)/D \\ b_{01} &= \left(\sum X_2^2 \sum Y_2 Y_1 - \sum X_2 Y_2 \sum X_2 Y_1\right)/D \\ b_{00} &= y_{1s} - b_{10}x_{2s} - b_{01}y_{2s} \end{aligned} \qquad (3)$$

where n is the number of control points, x,y are the coordinate components per control point and **X,Y** are the vectors of normalized coordinate components used for computation. Indices $i = 1,2$ refer to the control point coordinates in the reference erosion level and to the control point coordinates in the erosion level to be transformed. The least-squares approach not only minimizes errors of control point locations but also yields a measure for average control point misfit in x,y units (eq. 4):

$$m_p^2 = \frac{1}{n-3}\sum_{n=1}^{n}[(x_{1n} - a_{00} - a_{10}x_{2n} - a_{01}y_{2n})^2 + (y_{1n} - b_{00} - b_{10}x_{2n} - b_{01}y_{2n})^2] \qquad (4)$$

Correction for image rotation

At this stage, image centre point coordinates are registered to the reference coordinate system. Since sample shift usually comprises translation and rotation, the associated image first must be corrected for sample rotation. The centres of gravity ($g1$, $g2$) of both triangles ($p1-p3$ and $p4-p6$) yield a measure of the sample rotation against the sample stage coordinate system (this could be any pair of points; however, the centres of gravity conveniently average out errors in the estimation of triangle corner points). When all images making up an erosion series are acquired with a fixed position (e.g. image borders parallel with stage coordinate system x,y axes) the rotation between any given erosion level and the reference can be assessed as follows (Fig. 6). Let α be the angle between the line $g1-g2$ and the sample stage coordinate x-axis in the reference erosion level; let α' be the corresponding angle in an arbitrary erosion level. The sample rotation α'' in the arbitrary erosion level relative to the 'reference' erosion level is then (eq. 5):

$$\alpha = -\left(\arctan\frac{y_{g2}-y_{g1}}{x_{g2}-x_{g1}} - \arctan\frac{y_{g2'}-y_{g1'}}{x_{g2'}-x_{g1'}}\right) \quad (5)$$

Now the sample rotation can be balanced by a corresponding anti-rotation of the acquired images around their centres. In practice, this

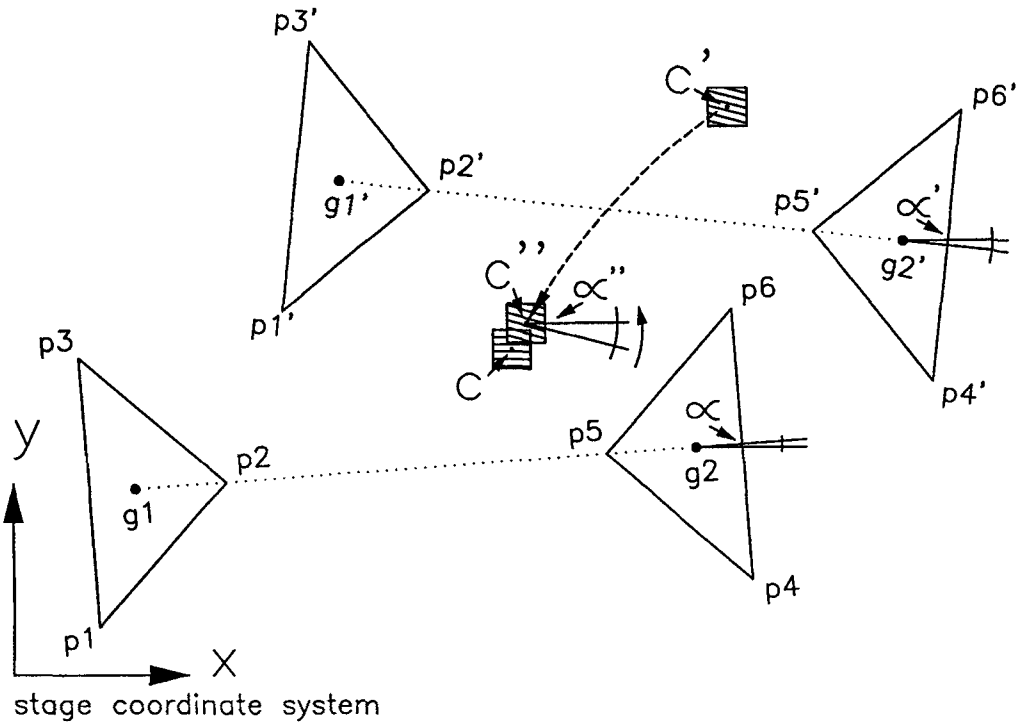

FIG. 6. Image centre coordinate registration and image correction for sample rotation. By means of polynomial transformation using control point pairs $p1-p1'$... $p6-p6'$, the image centre point c' is corrected for sample shifts and expressed in reference erosion level coordinates (c''; compare equations 3). Notice that sample shift both translates and rotates the sample under the acquisition system, which is calibrated to yield images with borders parallel to the sample stage coordinate system x, y axes. Since polynomial transformation is applied to correct image centre points only, associated images have to be internally anti-rotated for angle α'' (eq. 5) to correct for sample rotation. The sample rotation effect on image contents is depicted by hatching which runs parallel to sample stage x-axis in the reference erosion level. To illustrate these points, angles and shifts have been exaggerated. See text for more details.

image rotation is conveniently performed by the appropriate subroutine of an image processing package since the underlying resampling method should support nearest neighbour, bilinear or bicubic interpolation, depending on whether classified or raw images are to be processed (Foley *et al.*, 1991).

Correction for image shift

The image centre c″ still needs to be corrected for image shifts. Since c'' has been already transformed to reference erosion level coordinates and image rotation has been performed, image x,y shifts are equal to the coordinate x,y differences between c and c'' (Fig. 7). With respect to the image to be registered, coordinate differences have to be recalculated to image column and row shifts (eq. 6):

$$shift\_x = -\frac{x_c - x_{c''}}{pix\_x}; \qquad shift\_y = \frac{y_c - y_{c''}}{pix\_y} \quad (6)$$

where x_c, y_c, x_c', y_c'' are the coordinate components of image centres in the reference erosion level and in the erosion level to be corrected; *pix_x* and *pix_y* are the dimensions of pixels in sample stage coordinate units; *shift_x* and *shift_y* are the image-internal shiftings in terms of image columns and rows. Equations 5 and 6 refer to the specific stage and image coordinate system layout of the EPMA used in this study; they must be customized for different equipment. Figure 8 shows the result of applying the above corrections to the distorted data set shown in Fig. 2 for comparison. In Fig. 8 partially idiomorphic crystal faces are visible on the front side of the garnet and minor internal structures related to inclusions which are blurred in Fig. 2 can now be consistently traced between erosion levels. This example highlights the need for geometrical correction in order to achieve precise and consistent 3-D models from precision serial lapping and associated image acquisition.

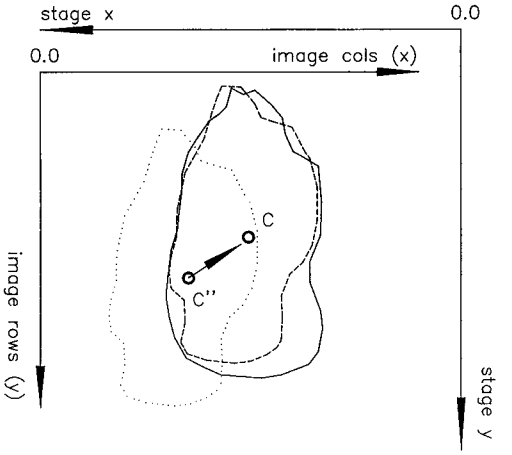

FIG. 7. Correction for image shifts by internal row/column shifting. Precise reference image centre relocation (c) by visual comparison is impossible. The changing shape of a hypothetical mineral grain in different erosion levels is indicated by solid outline (reference erosion level) and dotted outline (arbitrary erosion level). The image in an arbitrary erosion level (centre c'') has to be shifted internally to align the associated x,y coordinates with the image centre point in the reference erosion level. The dashed outline indicates the mineral outline in the arbitrary erosion level after geometrical correction. Notice the opposite direction of the x axes of the stage coordinate system and of the image column index of the JEOL 8600/LINK EXL system.

Other sources of geometrical errors

The correction of measurable geometrical shifts has been discussed above, but additional, small amounts of geometrical error are introduced by the finite precision of the optical reflection prisms. Further errors arise through the mislocation of the prisms' edges during coordinate extraction and through mechanical inaccuracies of the acquisition device's sample stage and the lapping device. In part, the magnitude of this induced inaccuracy is known, but in part it can only be indirectly estimated.

Mechanical precision of the lapping device

The following accuracy parameters apply to the precision lapping head used for this study: z-axis readout precision of the micrometer gauge ± 1 μm, precision of angular adjustment ± 2 minutes.

Mechanical precision of the sample stage

During the current study, for each prism edge $t1-t6$, two groups of 3 points, each located near the edge's ends, were picked and the related stage coordinates determined. Point location on the edges was performed by moving the prism edge

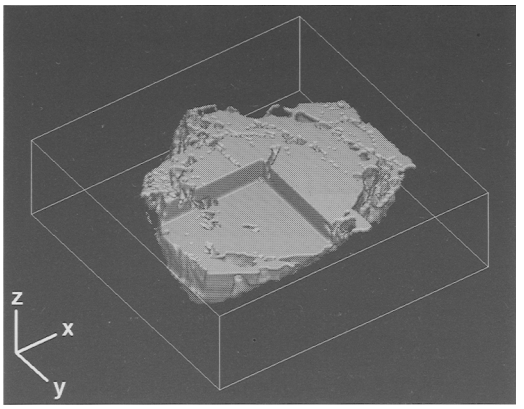

FIG. 8. Corrected 3-D visualization of the same garnet grain phase boundary as depicted in Fig. 2. The underlying 3-D model has been corrected using the procedures presented in this article. As compared with Fig. 2, the stair-effect caused by relative $x-y$ shifting of BSIs acquired at different erosion levels has been removed. Morphological details such as partially idiomorphic crystal faces and inclusion holes inside the garnet are now portrayed correctly.

exactly under the scanning screen's image centre mark (BSI mode, $\times 450$ magnification, compare Fig. 5). To check the overall accuracy of this referencing procedure, on one erosion level a reference prism was assessed ten times in the described way. From these data, the corresponding ten centres of gravity were calculated and statistically evaluated. Standard deviations in the x and y directions were 0.8 and 0.5 μm, respectively.

Angular accuracy of reflection prisms

The maximum error introduced by the reference prisms can be deduced from the manufacturer's stated tolerances. During the current study, reflection prisms with a height and side length of 16mm were used. The manufacturer's stated specification of angular tolerance of max. 8 minutes tilt out of orthogonality for prism faces relative to their bases can be calculated to cause a maximum error of 23 μm in the $x-y$ plane over the whole prism height (assuming the 'worst' case of all prism faces tilted to one side and taking the centre of gravity as a reference point). Reconstructing a garnet grain with x,y,z dimensions of approx. 1 mm (e.g. Fig. 1), a maximum $x-y$ distortion of 1.5 μm over the whole reconstruction height can be attributed to the prisms' geometrical inaccuracy. This influence can be neglected. However, even more accurately manufactured prisms are available if desired.

Precision of assemblage of the sample-internal reference system

The glass sample holder is an integral part of the sample internal reference system. Lapping its lower and upper surface ($s1$, $s2$ in Fig. 3) with the precision lapping head guarantees a highly plan-parallel substrate. Mounting prisms on this substrate by means of a bonding jig keeps the adhesive film between the glass holder and the prism's base surfaces below 1 μm (pers. comm. Logitech). Influences of these tilts upon the reference system precision are negligible in this context.

Bulk accuracy estimation

For the configuration described in this article, achievable geometrical accuracies of the resulting 3-D reconstructions are estimated as follows (expressed as ranges): ± 2 μm in model z-direction (lapping shift), ± 1.5μm in $x-y$ direction.

Practical referencing procedure

When performing the corrections described in this article in practice, it should be remembered that sample and image shift effects are counterbalanced by internally rotating and shifting the acquired images, i.e. applying proportionate row/column transformations to existing images. This necessitates, at any erosion level, an approximate relocation of the image centre point of the reference erosion level prior to image acquisition as well as using image sizes which allow for the maximum expected image shift (compare Fig. 1). To achieve this, the proposed method is as follows. When acquiring the reference erosion level image (usually the first erosion level), the position of the glass sample holder is marked on the acquisition device's sample stage. The area covered by the image is set to be larger than the maximum expected diameter of the mineral or fabric feature to be 3-D reconstructed. After each lapping stage, the sample is re-mounted according to the marks on the sample stage; this keeps sample shifts well below 1 mm and sample rotations below a few degrees. Image centre

points can then be coarsely relocated by automatically moving to the related positions on the reference erosion level and applying some manual position and focus corrections. Images are acquired and associated image centre coordinates are recorded. The stage coordinates of prism edges are recorded; all geometrical corrections are performed after image acquisition.

Another possible approach is to extract prism control points first, perform coordinate registration, automatically move the sample stage to the corrected positions and acquire the images. However, manual focusing followed by internal image rotation is still required. Moreover, elongated mineral grains which are inclined with respect to the erosion plane cannot be handled by this second approach because they tend to move out of the image at some erosion level.

In BSI mode, coordinates of points on the prism edges are extracted rapidly: locating the necessary 36 points (6 edges with three points located near each end) took approximately 15 minutes per erosion level. Regarding the necessary acquisition device, any SEM or EPMA providing a precise $x-y$ control and readout of the sample stage can be used for imaging. Simultaneous processing of several samples subject to 3-D reconstruction (i.e. mounting, as indicated in Fig. 4, two or more samples on one glass holder) minimizes the time spent for preparatory and referencing activities per sample, thus increasing the efficiency of 3-D microstructure reconstruction.

Conclusions

For reliable 3-D reconstruction of geological materials from precision serial lapping, a sample internal reference system is of paramount importance. Such a reference system can be conveniently assembled from optical reflection prisms, which are very precise, readily available and comparatively cheap. Besides a bonding jig, no specialized devices are necessary to set up this reference system. Since referencing physically relies on edges and not on corner points, the reference system is mechanically robust and derived coordinates are statistically more precise than coordinates retrieved from single points.

An AutoCAD based implementation of the correction procedures described in this article is available on request. More images and animations of geological microstructure reconstructions can be downloaded from the internet: http://www.sbg.ac.at/gew/leute/marsch/marsch_e.htm.

Acknowledgements

This work has been sponsored by the Austrian Academy of Science (APART grant) as well as by the Austrian Science Foundation (grant P-10858 GEO). D. Topa's acquisition work on the microprobe is highly appreciated as well as constructive discussion by N. Fortey, V. Höck and Ch. Stejskal.

References

Bryon, D.N., Atherton, M.P. and Hunter, R.H. (1995) The interpretation of granitic textures from serial thin sectioning, image analysis and three-dimensional reconstruction. *Min. Mag.*, **59**, 203–11.

Cooper, M.R. and Hunter, H.R. (1995) Precision serial lapping, imaging and three-dimensional reconstruction of minus-cement and post-cementation intergranular pore-systems in the Penrith Sandstone of north-western England. *Min. Mag.*, **59**, 213–20.

Denison, C. and Carlson, W.D. (1997) Three-dimensional quantitative textural analysis of metamorphic rocks using high-resolution computed X-ray tomography: Part II. Application to natural samples. *J. Metam. Geol.*, **15**, 45–57.

Foley, J.D., van Dam, A., Feiner, S.K. and Hughes, J.F. (1991) *Computer Graphics - Principles and Practice* (2nd ed.). Addison-Wesley, 1174 pp.

Göpfert, W. (1987) *Raumbezogene Informationssysteme*. Wichmann Karlsruhe, 278pp.

Grunsky, E.C., Robin, P.Y.F. and Schwerdtner, W.M. (1980) Orientation of Feldspar Porphyroclasts in Mylonite Samples from the Southern Churchill Province, Canadian Shield. *Tectonophysics*, **66**, 213–24.

Johnson, S.E. (1993) Unravelling the spirals: a serial thin-section study and three-dimensional computer-aided reconstruction of spiral-shaped inclusion trails in garnet prophyroblasts. *J. Metam. Geol.*, **11**, 621–34.

Marschallinger, R., Topa, D. and Höck, V. (1992) Three dimensional reconstruction of chemically zoned minerals by geostatistical interpolation of microprobe analysed serial sections. *Electron Microscopy*, Proc. EUREM 92, **I**, p. 449

Marschallinger, R., Höck, V. and Topa, D. (1993) A method for the 3-D reconstruction of chemically zoned minerals from microprobe scanned serial sections. *Eur. Microscopy Analysis*, **26**, 5–7.

Mather, P.M. (1989) *Computer Processing of Remotely-Sensed Images*. Wiley, Chichester, 352 pp.

Ohashi, Y. (1992) Three-dimensional reconstruction of pore geometry from serial sections: Image algebraic approach. In *Computer Graphics in Geology*.

Lecture Notes in Earth Sciences, 41, (R. Pflug and J.W. Harbaugh, eds.). Springer, 63–76.

Research Systems, Inc. (1995) *IDL Reference Guide*. RSI, Boulder CO, 1–2, 1173 pp.

Rock, N.M.S. (1988) *Numerical Geology. Lecture Notes in Earth Sciences, 18*, Springer, 427 pp.

[*Manuscript received 17 June 1997: revised 30 January 1998*]